Geotechnical Aspects of Underground Construction in Soft Ground – Yoo, Park, Kim & Ban (Eds)

Permanent increments of internal forces on a tunnel lining due to dynamic loadings

G. Lanzano
University of Molise, Campobasso, Italy

E. Bilotta
University of Napoli Federico II, Naples, Italy

ABSTRACT: The seismic design issues for shallow tunnel design are often poor or absent in the current national or international recommendations. Moreover, the available simplified formulations for the evaluation of tunnel internal forces, induced by seismic actions, account only for transient effects due to wave passage. Some centrifuge tests on circular tunnels in dry sand, recently performed, showed that permanent increments of internal forces clearly arise in the tunnel lining after seismic events. This evidence is also confirmed in real scale monitoring of tunnels, which suffered residual stresses after strong earthquakes. In order to capture the permanent increments of internal forces on a tunnel lining due to dynamic loadings, a series of numerical analyses have been performed by using a material model which includes hardening plasticity and the strain dependency of stiffness and damping. A experimental set of centrifuge tests in sand was used to validate the numerical analyses. The influence of the soil-lining relative stiffness and of the shear stress transmission at the interface between the soil and the lining are discussed in the paper.

1 INTRODUCTION

The seismic response of shallow circular tunnels in soft ground is generally safer compared to above ground structures; nevertheless, several tunnels suffered strong damage in recent earthquakes (Wang et al. 2001, Backblom & Munier 2002, Yoshida 2009). These can be associated with the onset of loading conditions incompatible with the lining resistance.

A number of existing methods permit to calculate the transient changes of internal forces in the lining during seismic shaking. They are generally based on the estimation of the seismic increment of shear strain at the tunnel depth (Wang, 1993; Penzien and Wu, 1998) or on linear equivalent visco-elastic numerical analyses of the dynamic soil-structure interaction (e.g. Lanzano et al. 2014a).

However, experimental and numerical evidences of permanent changes of internal loads in the tunnel lining have been collected (e.g. O'Rourke et. al. 2001; Amorosi & Boldini 2009; Lanzano et al. 2012) suggesting that soil-structure interaction should be ideally modeled to capture such effects, by accounting for soil plastic straining under cyclic loading. Rarely such analyses are performed in the conventional design.

At the 7th International Symposium on Geotechnical Aspects of Underground Construction in Soft Ground held in Rome in 2011 a predictive exercise was launched (Bilotta & Silvestri 2012, 2013) aimed at involving several research groups in modeling such a problem. Many groups carried out the exercise and obtained interesting results (*cf.* Tsinidis et al. 2014; Hleibieh et al. 2014; Conti et al. 2014; Gomes 2014; Amorosi et al. 2014, Bilotta et al. 2014a).

In the work presented in this paper a series of numerical analyses have been performed by using a material model which includes hardening plasticity and the strain dependency of stiffness and damping (Benz, 2008), in order to capture the permanent increments of internal forces on a tunnel lining due to dynamic loadings. The experimental set of centrifuge tests in sand (Lanzano et al. 2010, 2012) was used to validate the numerical analyses. The influence of the soil-lining relative stiffness and of the shear stress transmission at the interface between the soil and the lining are discussed.

2 EXPERIMENTAL BENCHMARK

The experimental campaign used as benchmark for the numerical study presented in this paper is presented in Lanzano et al. (2012) and shortly described in another paper presented at this symposium (Bilotta et al. 2014b), therefore it will not be repeated here. It consists of four centrifuge tests on tunnel model in dry sand, which underwent pseudo-harmonic loadings.

A schematic layout of the tests is shown in Figure 1, with the position of the measuring

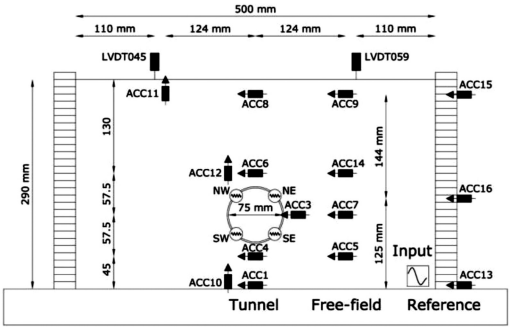

Figure 1. Layout of Model T3.

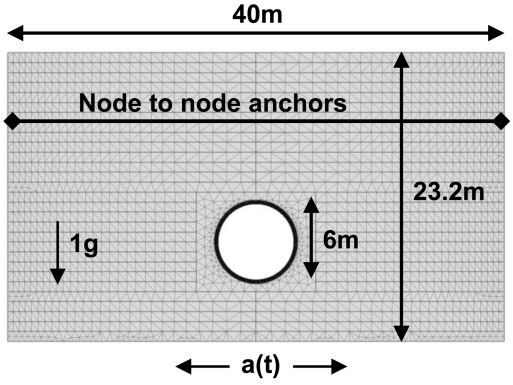

Figure 2. Mesh for the numerical analyses (prototype scale).

devices: accelerometers embedded at several locations; LDVTs at the model surface; strain gauges on the tunnel lining.

The experimental behavior observed in the centrifuge tests was reproduced in a reference set of finite element analyses, both at the same scale of the tests (model scale) and at the real scale (prototype scale) by applying the appropriate scaling laws. Further, numerical modeling has been extended, at the prototype scale only, to investigate the influence on the internal forces calculated in the lining of some relevant geometrical and mechanical parameters (small-strain soil stiffness, lining stiffness, interface behavior). The relevant scaling laws can be found in Madabhushi (2014).

3 NUMERICAL ANALYSES

3.1 *Model vs. prototype*

The numerical analyses were carried out using the commercial code Plaxis 2D (Brinkgreve et al. 2011). This is a commercial FEM code, which solves the motion equations in the time domain. The mesh adopted at the prototype scale is shown in Fig. 2.

A *node-to-node* constraint has been used (1 mm vertical spacing) in order to simulate the laminar box behavior during the shaking (Bilotta et al. 2009). A lithostatic distribution of the horizontal stress has been provided at the lateral boundaries of the model.

Table 1. Input parameters for reference numerical analyses.

E_{50} (MPa)	12
E_{oed} (MPa)	8.6
E_{ur} (MPa)	44.8
m (−)	0.25
G_0 (MPa)	60
$\gamma_{0.7}$(−)	$5.8 \cdot 10^{-4}$
ϕ_{PC} (°)	38.6
ψ_{PC} (°)	8.2
c (kPa)	0.01

Table 2. Earthquakes fired in test T3 (prototype scale).

earthquake #	1	2	3	4
main frequency (Hz)	0.375	0.5	0.625	0.75
duration (s)	32	32	32	32
nominal PGA (g)	0.05	0.10	0.12	0.15

The tunnel (diameter $D = 6\,m$) was modeled as a linear elastic beam ($EI = 3.7 \cdot 10^2\,kNm^2/m$; $EA = 2.8 \cdot 10^6\,kN/m$). A very smooth interface was considered between the lining and the ground, by using an interface factor $R_{inter} = 0.05$. Lanzano et al. (2014a) observed that this value returned the best agreement between numerical and experimental values of dynamic increments of hoop force.

The sand was modeled using the Hardening Soil Small Strain model (cf. Benz, 2008). The calibration of the model mechanical parameters was performed by using the results of laboratory volume element tests (triaxial and torsional shear tests) and by back-analyzing the available centrifuge tests, as discussed in Lanzano et al. (2014b). In Table 1, the main significant model parameters are shown. In Table 2, the characteristics of the input pseudo-harmonic signals applied at the base are summarized (prototype scale).

In Figure 3 and 4 a comparison among the experimental evidences and the numerical results at model and prototype scale is presented in terms of accelerations time histories and response spectra at the top of the reference array. For the sake of comparison, here and in the following the experimental results and the calculations at model scale are scaled up at the prototype scale.

Both at the model and at the prototype scale the numerical predictions are satisfactory. The main features of the experimental data are well reproduced, both in terms of amplitude of acceleration time history and of frequency content.

Figure 5 shows a comparison between experimental and numerical time histories of surface settlement. The numerical predictions are both at model and at prototype scale.

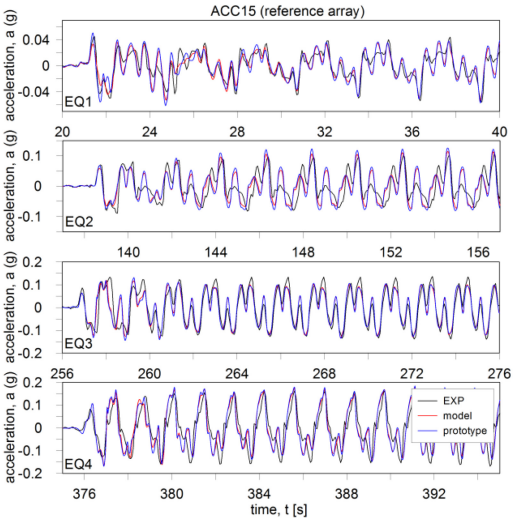

Figure 3. Acceleration time histories.

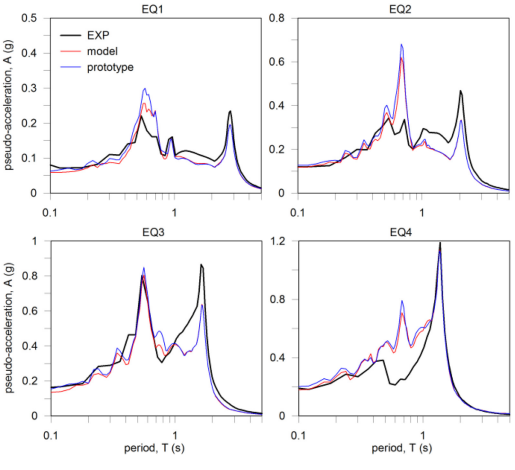

Figure 4. Pseudo-acceleration spectra.

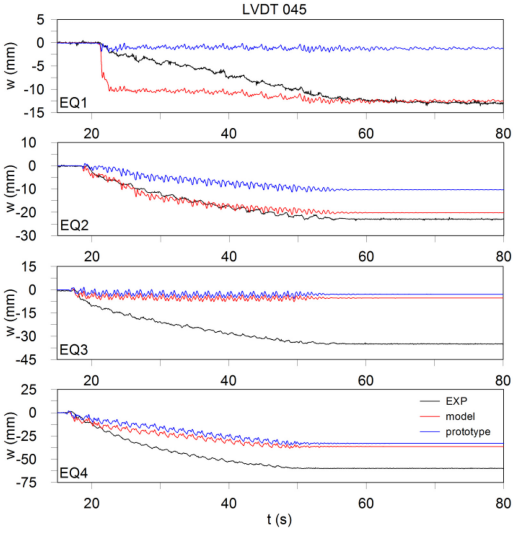

Figure 5. Surface settlements.

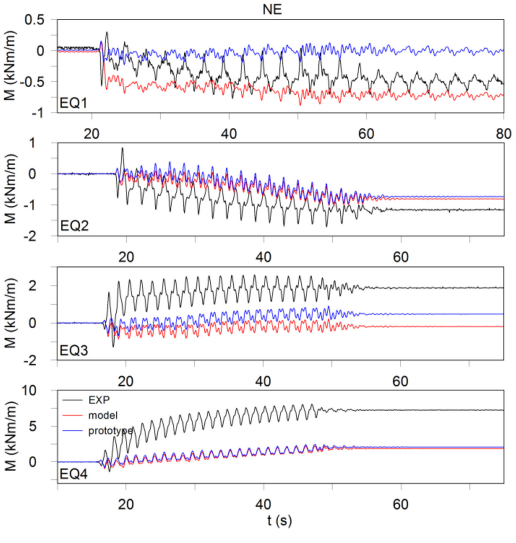

Figure 6. Bending moments.

Densification of the sand layer is clearly noted in the experiments and reproduced by the analyses. A rather high difference between the computations at model and prototype scale can be observed for the first and the second shaking event (EQ1 and EQ2). It is worth noting that such a difference between the predictions does not affect the reversible (cyclic) component of settlement. This is quite similar in both analyses and very close to the experimental measurements. Larger differences arise instead among the cumulated settlement, which is generally larger in the tests and lower in the computations at the prototype scale.

Experimental and numerical time histories of bending moments are shown in Figure 6. Consistently to what observed in settlement time histories, the prediction of the reversible component of bending moment during shaking is close to the relevant experimental measurements. On the other hand, since densification is not always well reproduced, differences arise among numerical predictions and experimental measurements of residual bending moments in the lining.

A similar comparison is shown in the plots of Figure 7 for the time histories of hoop force.

It may be noticed a larger difference between the two numerical predictions (at model and at prototype scale) of residual hoop forces, being in this case the predictions at the prototype scale closer to the experimental data. However, the increments of hoop forces during and after shaking seem negligible if compared to the corresponding static values.

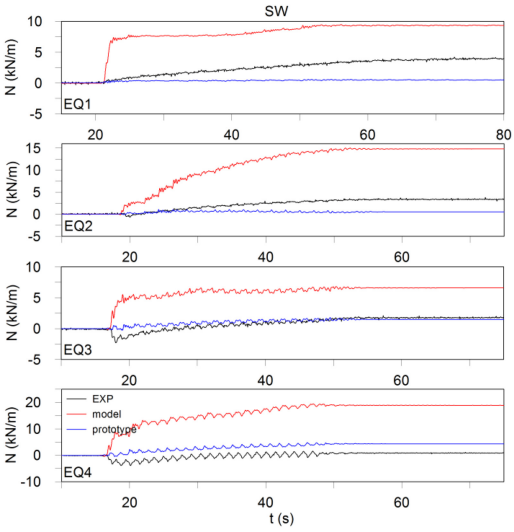

Figure 7. Hoop forces.

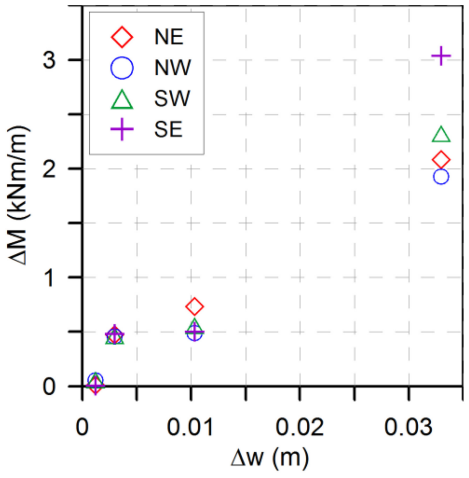

Figure 8. Accumulated bending moment ΔM *vs* vertical surface settlement Δw ($EI = 3.7 \cdot 10^2$ kNm^2/m; $EA = 2.8 \cdot 10^6$ kN/m; $R_{inter} = 0.05$).

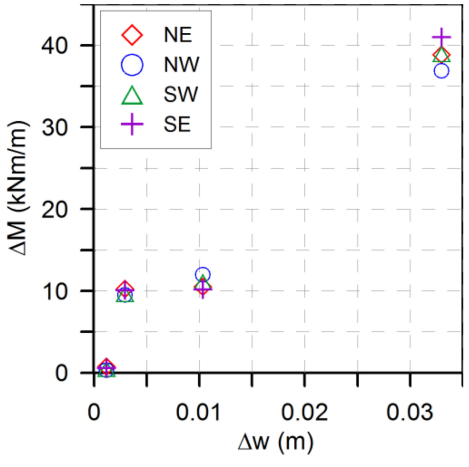

Figure 9. Accumulated bending moment ΔM *vs* vertical surface settlement Δw ($EI = 7.1 \cdot 10^4$ kNm^2/m; $EA = 9.5 \cdot 10^6$ kN/m; $R_{inter} = 0.05$).

3.2 *Parametric analyses*

A series of parametric analyses were then carried out starting from the reference configuration at true scale (§3.1). The flexural and axial stiffness were changed to simulate more rigid linings such as those adopted for urban underground railways and made of reinforced concrete. The shear stress transmission at the interface between the lining and the ground was also changed towards more realistic values.

The results in terms of accumulated bending moments during each earthquake are shown in the followings for the lining of the reference analysis and a reinforced concrete lining ($EI = 7.1 \cdot 10^4$ kNm^2/m; $EA = 9.5 \cdot 10^6$ kN/m) with a very smooth ($R_{inter} = 0.05$) and a normally rough interface ($R_{inter} = 0.7$).

An almost linear trend of the accumulated bending moment with surface settlement (calculated at the position of LVTD 045 in the test, *cf.* Fig. 1) can be observed in Figure 8 for the reference analysis ($EI = 3.7 \cdot 10^2$ kNm^2/m; $EA = 2.8 \cdot 10^6$ kN/m; $R_{inter} = 0.05$). The plotted values were calculated in in the same positions of the measurements in the test (strain gauges in Fig. 1).

A similar dependency of the accumulation of bending moment in the lining with the sand densification can be observed in Figure 9, where a plot [Δw, ΔM] is shown for the reinforced concrete lining, assuming a very smooth interface ($EI = 7.1 \cdot 10^4$ kNm^2/m; $EA = 9.5 \cdot 10^6$ kN/m; $R_{inter} = 0.05$). Since the flexural stiffness is higher the bending moments are one order of magnitude higher than those shown in Figure 8.

Finally the same kind of plot is shown in Figure 10 for the case of reinforced concrete lining with a realistic interface ($EI = 7.1 \cdot 10^4$ kNm^2/m; $EA = 9.5 \cdot 10^6$ kN/m; $R_{inter} = 0.7$). Even larger values of accumulated bending moment are calculated in this case. At least for the more severe event such values are of the same order of magnitude of typical values of bending moment under static conditions.

Accumulated hoop forces are shown for the latter case only ($EI = 7.1 \cdot 10^4$ kNm^2/m; $EA = 9.5 \cdot 10^6$ kN/m; $R_{inter} = 0.7$) in Figure 11. In such conditions the accumulation of hoop forces is not negligible compared to the pre-existing static values, particularly for the stronger event (EQ4).

For the case of reinforced concrete lining with a realistic interface ($EI = 7.1 \cdot 10^4$ kNm^2/m; $EA = 9.5 \cdot 10^6$ kN/m; $R_{inter} = 0.7$) the distributions of bending moments and hoop forces in the static conditions and after each seismic event are shown in Figures 12 and 13.

It can be noticed that as far as the tunnel undergoes further shaking the bending moments along the cross

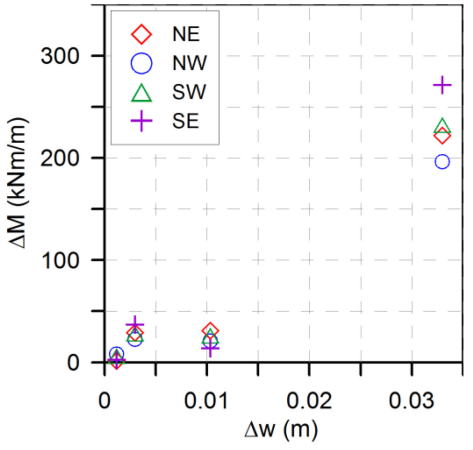

Figure 10. Accumulated bending moment ΔM *vs* vertical surface settlement Δw ($EI = 7.1 \cdot 10^4$ kNm^2/m; $EA = 9.5 \cdot 10^6$ kN/m; $R_{inter} = 0.7$).

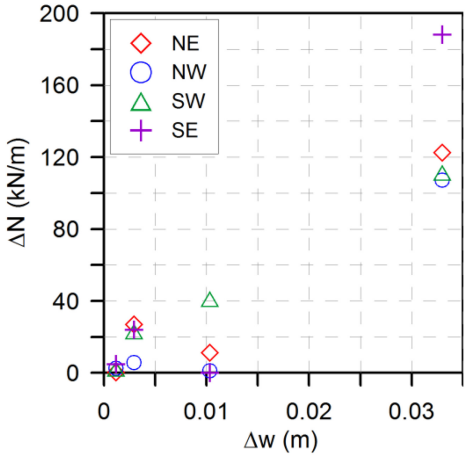

Figure 11. Accumulated hoop force ΔN *vs* vertical surface settlement Δw ($EI = 7.1 \cdot 10^4$ kNm^2/m; $EA = 9.5 \cdot 10^6$ kN/m; $R_{inter} = 0.7$).

section increase. After the last event (EQ4) the value of bending moment is considerably higher compared to the initial static conditions. By comparing Fig. 12 to Fig. 10, one may conclude that, depending on the intensity of shaking, an average bending moment up to two-three times larger than the maximum static value was calculated.

The average change of hoop force (cf. Fig. 11) is instead rather low (even after EQ4) compared to the initial static value (cf. Figure 13).

Overall, after the seismic events a general increase of the working load of the structural section is expected. In this case, the hypothesis of linear elasticity adopted for the structural elements should be removed to refine the results.

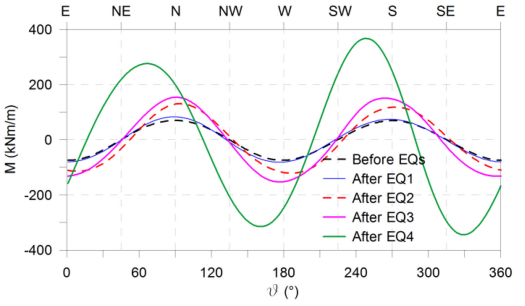

Figure 12. Distribution of bending moment M around the tunnel section ($EI = 7.1 \cdot 10^4$ kNm^2/m; $EA = 9.5 \cdot 10^6$ kN/m; $R_{inter} = 0.7$).

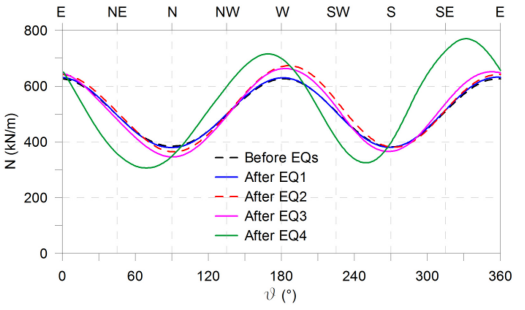

Figure 13. Distribution of hoop force N around the tunnel section ($EI = 7.1 \cdot 10^4$ kNm^2/m; EA=$9.5 \cdot 10^6$ kN/m; $R_{inter} = 0.7$).

4 CONCLUSIONS

The simplified formulations for the evaluation of seismic induced internal forces in the transverse section of a tunnel lining account only for transient effects due to wave passage. Experimental evidences of permanent changes of internal loads in the tunnel lining exist, which are not predictable with the commonly adopted elastic approach. In this paper the results of a series of numerical analyses carried out by using for soil a material model which includes hardening plasticity and the strain dependency of stiffness and damping are shown.

The results of the analyses have been compared to the experimental results of centrifuge tests on sand models and they show how the accumulation of irreversible components of bending moment and hoop force in the tunnel lining is pretty much dependent on the sand densification. The surface settlement can be assumed as a global marker of the volumetric plastic strain due to shaking. An almost linear dependence of the increment of bending moment and hoop force on the surface settlement was observed.

In particular for a typical geometry of urban railways tunnels, the increase of working loads in the lining at the end of shaking may be not negligible compared to the previous static conditions.

REFERENCES

Amorosi A., Boldini D. 2009. Numerical modelling of the transverse dynamic behaviour of circular tunnels in clayey soils, *Soil Dynamics and Earthquake Engineering*, 29, 1059–1072.

Amorosi A., Boldini D., Falcone G. 2014. Numerical prediction of tunnel performance during centrifuge dynamic tests. *Acta Geotech* doi: 10.1007/s11440-013-0295-7.

Bäckblom G., Munier R. 2002. Effects of earthquakes on the deep repository for spent fuel in Sweden based on case studies and preliminary model results, *Technical Report TR-02-24*, Swedish Nuclear Fuel and Waste Management Co.

Benz T. 2008. Small-strain stiffness and its numerical consequences. PhD Thesis, University of Stuttgart.

Bilotta E., Lanzano G., Madabhushi S.P.G., Silvestri F. 2014. A Round Robin on Tunnels Under Seismic Actions *Acta Geotechnica*, doi: 10.1007/s11440-014-0330-3.

Bilotta E., Lanzano G., Russo G., Silvestri F., Madabhushi S.P.G. 2009. Seismic analyses of shallow tunnels by dynamic centrifuge tests and finite elements. *Proc 17th Int Conf on Soil Mechanics and Geotechnical Engineering*, Alexandria, Egypt, Balkema.

Bilotta E., Madabhushi S.P.G., Silvestri F. 2014. Otcomes of RRTT, a predictive exercise on the behavior of tunnels under seismic actions. *8th Int Symp on Geotech Aspects of Underground Construction in Soft Ground*.

Bilotta E., Silvestri F. 2012. A predictive exercise on the behaviour of tunnels under seismic actions. *Proc IS-Roma 2011 7th Int Symp Geotech Aspects of Underground Construction in Soft Ground*. CRC Press 1071–1077.

Bilotta E., Silvestri F. 2013. A round robin test on tunnels under seismic actions. *Geotech News* 31(1):40–44.

Brinkgreve R.B.J., Swolfs W.M., Engin E. 2011. Plaxis 2D Manual.

Brinkgreve R.B.J., Kappert M.H., Bonnier P.G. 2007. Hysteretic damping in a small-strain stiffness model. *Proc. of Num. Mod. in Geomech., NUMOG X, Rhodes*, 737–742.

Conti R., Viggiani G.M.B., Perugini F. 2014. Numerical modelling of centrifuge dynamic tests of circular tunnels in dry sand. *Acta Geotech* doi:10.1007/s11440-013-0286-8.

d'Onofrio, A, Silvestri, F, Vinale, F, 1999. New torsional shear device, *Geotechnical Testing Journal*, 22(2), 107–117.

Gomes R.C. 2014. Numerical simulation of the seismic response of tunnels in sand with an elastoplastic model. *Acta Geotech* doi:10.1007/s11440-013-0287-7.

Hashash Y.M.A., Park D., 2002. Viscous damping formulation and high frequency motion propagation in non-linear site response analysis. *Soil Dynamics and Earthquake Engineering*, 22: 611–624.

Hleibieh J., Wegener D., Herle I. 2014. Numerical simulation of a tunnel surrounded by sand using a hypoplastic model. *Acta Geotech* doi: 10.1007/s11440-013-0294-8.

Lanzano G., Bilotta E., Russo G., Silvestri F. 2014. Experimental and numerical study on circular tunnels under seismic loading. *Eur J of Environm and Civil Eng* doi: 10.1080/19648189.2014.893211.

Lanzano G., Bilotta E., Russo G., Silvestri F., Madabhushi S.P.G. 2010. Dynamic centrifuge tests on shallow tunnel models in dry sand. *Proc. of the 7th International Conference on Physical Modelling in Geotechnics*, 1, 561–567.

Lanzano G., Bilotta E., Russo G., Silvestri F., Madabhushi S.P.G. 2012. Centrifuge modeling of seismic loadings on tunnels in sand, *ASTM Geotechnical Testing Journal*, 35 (6): 854–869.

Lanzano G., Santucci de Magistris F., Bilotta E. 2014. Calibration of the mechanical parameters for the numerical simulations of dynamic centrifuge experiments. *Proc. of the 8th European Conference on Numerical Methods in Geotechnical Engineering, Delft, 18–20 June*.

Madabhushi, S.P.G., (2014), Centrifuge modelling for Civil Engineers, Spon Press, ISBN-10: 0415668247.

O'Rourke, T. D., Goh, S. H., Menkiti, C. O., Mair, R. J. 2001. Highway Tunnel Performance during the 1999 Duzce Earthquake, *Proc. 15th International Conference on Soil Mechanics and Geotechnical Engineering, Istanbul, Turkey, 1365–1368.*

Penzien J., Wu, C.L. 1998. Stresses in linings of bored tunnels, Earthquake Engineering and Structural Dynamics, 27, 283–300.

Tsinidis G., Pitilakis K., Trikalioti D. 2014. Numerical simulation of round robin numerical test on tunnels using a simplified kinematic hardening model. *Acta Geotech* doi:10.1007/s11440-013-0293-9.

Wang W.L., Wang T.T., Su J.J., Lin C.H., Seng C.R., Huang T.H. 2001. Assesment of damage in mountain tunnels due to the Taiwan Chi-Chi earthquake, *Tunnelling and Underground Space Technology*, 16, 133–150.

Wang, J-N. 1993. *Seismic Design of Tunnels*, Parson Brinckerhoff Inc.

Yoshida N. 2009. Damage to subway station during the 1995 Hyogoken-Nambu (Kobe) earthquake, *Earthquake geotechnical case histories for performance-based design*, (Kokusho Ed)., 373–389.